Structure and thermodynamics of the dipolar hard sphere fluid from the reference-hypernetted chain equation with minimized free energy

F. Lado
Physics Department, North Carolina State University, Raleigh, North Carolina 27695-8202

M. Lombardero
Instituto de Química Física Rocasolano, C.S.I.C. Serrano 119, and Departmento de Química Física, Facultad de Química, Universidad Complutense, 28040 Madrid, Spain

E. Enciso, S. Lago, and J. L. F. Abascal
Departamento de Química Física, Facultad de Química, Universidad Complutense, 28040 Madrid, Spain

(Received 10 February 1986; accepted 13 May 1986)

The reference-hypernetted chain equation, generalized to molecular fluids, is optimized by choosing the reference system so as to minimize the free energy. This procedure, which assures a significant improvement in the internal thermodynamic consistency of the theory, is here applied to a fluid of dipolar hard spheres, using both the complete dipolar potential and one with a reaction field (RF) truncation. We confirm that a recent reformulation of the relation between the dielectric constant ϵ and the mean square dipole moment for the RF geometry indeed brings ϵ for the truncated potential into reasonably good agreement with the infinite-range values, but that the important correlation functions nevertheless differ qualitatively in their long-range behavior. The method of solving the molecular integral equation, developed earlier, can be applied to other multipolar potentials, or alternatively, to molecules with distributed point charges.

I. INTRODUCTION

The reference-hypernetted chain (RHNC) integral equation,[1] broadened in its scope by the Rosenfeld–Ashcroft[2] insight of an *adjustable* reference system, and optimized by requiring this adjustment to minimize the free energy,[3] has proved to be a versatile and reliable tool in the study of simple fluids.[3,4] The formal generalization of the same procedure to molecular fluids is straightforward[5]; as yet, however, no actual calculation for anisotropic potentials has been carried out using this prescription. In this paper, we report the results of applying the optimized RHNC equation to a fluid of dipolar hard spheres.

To the usual difficulties of dealing with the additional degrees of freedom in molecular systems, particles with dipolar interactions add a special problem of their own, that of coping numerically with the comparatively long-ranged nature of this potential. This is particularly troublesome for numerical simulation studies, which most often adapt themselves to the finiteness of the simulated sample by truncation of the intermolecular potential and imposition of toroidal boundary conditions. Ironically, the macroscopic property of central interest for dipolar models, the dielectric constant ϵ, turns out to be very sensitive to such modifications, with the result that not only has there been some controversy over the correct way to compute ϵ in finite geometries so as to simulate bulk values, but in practice the values of ϵ that have been reported show discouraging scatter.[6] More recently, rigorous expressions connecting ϵ with the equilibrium dipole moment fluctuations in truncated geometries such as the reaction field method have been derived.[7,8] Nevertheless, for the dipolar potential, computer simulation methods have so far played something less than their usual role as makers of touchstones.

Integral equations, on the other hand, can easily deal with such long-range functions as the dipolar potential; their shortcoming instead is that they are inherently approximate, often to an unknown extent until their results can be systematically contrasted with those of simulation studies. In the present context of complementary weaknesses, however, a reliable approximate integral equation can be a valuable aid to the simulation techniques themselves, in that it can provide an independent testbed for the study of the effects of the inevitable modifications of the model potential that the latter must accept. A small effort in this direction is included in this paper.

Recently, Fries and Patey[9] have reported data obtained from the RHNC equation (without optimization) for three thermodynamic states of dipolar hard spheres. They find the results to be in much better agreement with simulation data than those of several earlier theories, especially for the dielectric constant. Here we repeat these calculations for comparison. We further obtain the solution of the optimized RHNC equation for a larger collection of thermodynamic states, using both the complete dipolar potential and the simulation version with reaction field (RF) truncation. In brief, we find that the (presumed) improvements from the optimization condition, here applied to a hard sphere reference system, mainly appear in the mechanical quantities of pressure and compressibility, with the dielectric constant being scarcely affected. Furthermore, we confirm that the recent RF formula for ϵ[7,8] brings its value into consonance with that of infinite samples (provided the cutoff distance is large enough), while the correlation functions using RF truncation nonetheless display anomalous long-range behavior.

For the sake of minimal completeness, Sec. II contains a

 0021-9606/86/172916-06$02.10

brief outline of the algorithm[10] used to solve the optimized RHNC equation. (We note that essentially the identical procedure can be applied to other multipolar potentials, or alternatively, to molecules with distributed point charges, as well as to molecules with nonspherical cores.[11]) The results of the calculation for dipolar hard spheres are given in Sec. III.

II. PROCEDURE

The numerical task at hand is to solve the Ornstein–Zernike (OZ) equation

$$S(12) = \frac{\rho}{4\pi} \int d\mathbf{r}_3 d\omega_3 C(13)[S(32) + C(32)] , \quad (1)$$

coupled with the RHNC closure

$$C(12) = \exp[-\beta\phi(12) + S(12) + B_0(12)] - 1 - S(12) \quad (2)$$

for the series function $S(12)$ and the direct correlation function (DCF) $C(12)$. [The potential $\phi(12)$ and the reference bridge function $B_0(12)$ are assumed to be given. They are discussed below.] With a solution in hand we may then construct the pair distribution function (PDF)

$$g(12) = \exp[-\beta\phi(12) + S(12) + B_0(12)] , \quad (3)$$

and determine the thermodynamics of the molecular fluid at density ρ and temperature $T = 1/k_B\beta$ through standard quadratures.

The pair functions such as $S(12)$ for linear molecules in these equations depend in general on the separation $\mathbf{r}_{12}$ between the molecular centers of mass and on the orientations $\omega_1 = (\theta_1,\phi_1)$ and $\omega_2 = (\theta_2,\phi_2)$ of the two molecular axes referred to some arbitrary coordinate frame,

$$S(12) = S(\mathbf{r}_{12},\omega_1,\omega_2) . \quad (4)$$

The simplest such representation results from the choice of $\mathbf{r}_{12}$ as the z axis of the coordinate frame, for which now

$$S(12) = S(r_{12},\theta_1,\theta_2,\phi_{12}) \quad (5)$$

can be expanded in spherical harmonics as[12]

$$S(12) = 4\pi \sum_{l_1,l_2,m} S_{l_1l_2m}(r_{12}) Y_{l_1m}(\omega_1) Y_{l_2\bar{m}}(\omega_2) , \quad (6)$$

where $\bar{m} = -m$ and $\phi_{12} = \phi_1 - \phi_2$. The calculation is then to determine a finite but sufficient set of the axial $S_{l_1l_2m}(r)$ projections. Other orientation-dependent functions are handled similarly.

The solution of the nonlinear equations (1) and (2) is by iteration; the steps constituting one iteration are outlined below. For a more complete presentation of this procedure, as well as additional references, the interested reader is referred to Ref. 10.

(i) Compute the DCF coefficients

From the current set of $S_{l_1l_2m}(r)$ coefficients we construct the set

$$C_{l_1l_2m}(r) = g_{l_1l_2m}(r) - \delta_{l_1l_2m,000} - S_{l_1l_2m}(r) , \quad (7)$$

using Eqs. (2) and (3), where

$$g_{l_1l_2m}(r) = \frac{1}{4\pi} \int d\omega_1 d\omega_2 g(12) Y^*_{l_1m}(\omega_1) Y^*_{l_2\bar{m}}(\omega_2) \quad (8)$$

is evaluated with n-point Gaussian quadratures as

$$g_{l_1l_2m}(r) = \frac{1}{n} \sum_{k_1,k_2,j} w_{k_1} w_{k_2} g(r,x_{k_1},x_{k_2},y_j) \times \mathscr{P}_{l_1m}(x_{k_1}) \mathscr{P}_{l_2m}(x_{k_2}) (-1)^m T_m(y_j) . \quad (9)$$

Here x_k and y_j are the n zeros of the Legendre polynomial $P_n(x)$ and Chebyshev polynomial $T_n(y)$, respectively, the weights w_k are

$$w_k = \{(1-x_k^2)[P'_m(x_k)]^2\}^{-1} , \quad (10)$$

and $\mathscr{P}_{lm}(x)$ is the associated Legendre function normalized to 2. The full angular dependence of $g(12)$ is obtained through Eq. (3), with $S(12)$ reconstructed from its coefficients using Eq. (6), which now reads

$$S(r,x_1,x_2,y) = \sum_{l_1,l_2,m} S_{l_1l_2m}(r) \mathscr{P}_{l_1m}(x_1) \mathscr{P}_{l_2m}(x_2) (-1)^m T_m(y) . \quad (11)$$

In the present calculation, the dipolar potential is similarly represented while the reference bridge function $B_0(12)$ has only a spherically symmetric term (see below). All r-dependent functions are evaluated at the points $r_j = j\Delta r$, $j = 1,2,\ldots,N_r - 1$.

(ii) Convert to space-fixed frame

The OZ equation is deconvoluted using Fourier transformation. To compute the Fourier transform of $C(12)$ we must represent it in some coordinate frame other than the axial one. This amounts to generating a new set of space-fixed coefficients from the axial ones by a Clebsch–Gordon (CG) transformation,

$$C(r;l_1l_2l) = \left(\frac{4\pi}{2l+1}\right)^{1/2} \sum_m \langle l_1 m l_2 \bar{m} | l_1 l_2 l 0 \rangle C_{l_1l_2m}(r) , \quad (12)$$

where the angular brackets are Clebsch–Gordon coefficients.

(iii) "Lower" the $l > 0$ members

The Fourier transform of $C(r;l_1l_2l)$ involves a spherical Bessel function kernel $j_l(kr)$. To avoid the complexity of several different transform algorithms, those coefficients with $l > 0$ are first "lowered" to new functions $C^{(0)}(r;l_1l_2l)$, which can be transformed with a $j_0(kr)$ kernel, by repeated application of

$$C^{(k-2)}(r;l_1l_2l) = C^{(k)}(r;l_1l_2l) - (2k-1) r^{k-2} \times \int_r^\infty dx \frac{C^{(k)}(x;l_1l_2l)}{x^{k-1}} , \quad (13)$$

starting from $C^{(l)}(r;l_1l_2l) \equiv C(r;l_1l_2l)$. In the present calculation, the coefficients of $C(12)$ have a finite discontinuity at the core diameter which must be taken into account in evaluating Eq. (13). The trapezoidal rule is used to evaluate the integral.

(iv) Compute Fourier transforms

The transforms

$$\tilde{C}(k;l_1l_2l) = 4\pi \int_0^\infty dr\, r^2 C^{(0)}(r;l_1l_2l) j_0(kr) \tag{14}$$

are computed using the fast Fourier transform (FFT). At the core discontinuity, $C^{(0)}(r;l_1l_2l)$ is assigned its mean value. Fourier transforms are determined at the points $k_j = j\pi/N_r\Delta r, j = 1,2,...,N_r - 1$.

(v) Convert to axial frame

Having obtained the transform of $C(12)$, we must now solve the OZ equation for the transform of $S(12)$. This turns out to be simpler if done in terms of an axial set of coefficients, with $\mathbf{k}$ as the z axis. Thus, we perform another Clebsch–Gordon transformation [the inverse of Eq. (12)] to generate the set

$$\tilde{C}_{l_1l_2m}(k) = \sum_l \langle l_1 m l_2 \bar{m} | l_1 m l_2 l 0\rangle \left(\frac{2l+1}{4\pi}\right)^{1/2} \tilde{C}(k;l_1l_2l) . \tag{15}$$

(vi) Solve the OZ equation for $\tilde{S}(12)$

The solution of the OZ equation is now effected as a set of matrix equations,

$$\tilde{\mathbf{S}}_m(k) = (-1)^m \rho [\mathbf{I} - (-1)^m \rho \tilde{\mathbf{C}}_m(k)]^{-1} [\tilde{\mathbf{C}}_m(k)]^2 , \tag{16}$$

where the matrices $\tilde{\mathbf{S}}_m(k)$, $\tilde{\mathbf{C}}_m(k)$ have elements $\tilde{S}_{l_1l_2m}(k)$, $\tilde{C}_{l_1l_2m}(k)$, respectively, with $l_1, l_2 \geqslant m$.

(vii) Convert to space-fixed frame

We now seek to Fourier invert $\tilde{S}(12)$ to get $S(12)$. Again, this requires a nonaxial frame of reference, so the axial coefficients $\tilde{S}_{l_1l_2m}(k)$ are converted to a space-fixed set through another CG transformation,

$$\tilde{S}(k;l_1l_2l) = \left(\frac{4\pi}{2l+1}\right)^{1/2} \sum_m \langle l_1 m l_2 \bar{m} | l_1 l_2 l 0\rangle \tilde{S}_{l_1l_2m}(k) . \tag{17}$$

(viii) Compute inverse Fourier transforms

We can now perform the Fourier inversion to get

$$S^{(0)}(r;l_1l_2l) = \frac{1}{2\pi^2} \int_0^\infty dr\, r^2 \tilde{S}(k;l_1l_2l) j_0(kr) \tag{18}$$

using again the FFT algorithm.

(ix) "Raise" the $l > 0$ members

As the inverse of Eq. (14), Eq. (18) generates the lowered version of the $S(12)$ coefficients. These must next be raised by the inverse of the operation in Eq. (13). This is

$$S^{(k)}(r;l_1l_2l) = S^{(k-2)}(r;l_1l_2l) - \frac{2k-1}{r^{k+1}} \int_0^r dx\, x^k S^{(k-2)}(x;l_1l_2l) , \tag{19}$$

applied recursively until reaching $k = l$. To avoid magnifying quadrature errors at small r upon dividing by r^{k+1}, the integral in Eq. (19) is evaluated using a modified trapezoidal rule, whereby only $S(x)$ is fitted by linear interpolation.

(x) Convert to axial frame

The final step completing one iteration is to generate the new axial projections of $S(12)$ by a CG transformation like that of Eq. (15),

$$S_{l_1l_2m}(r) = \sum_l \langle l_1 m l_2 \bar{m} | l_1 l_2 l 0\rangle \left(\frac{2l+1}{4\pi}\right)^{1/2} S(r;l_1l_2l) . \tag{20}$$

Here a test is made of the differences between the new and old axial coefficients of $S(12)$; if they are not small enough, we return to step (i). To speed the convergence, we have adopted Gillan's[13] method of performing Newton–Raphson iterations, but for simplicity only for the dominant radial term $S_{000}(r)$. Broyles' method of mixing iterates[14] is also helpful in coaxing convergence in the more stubborn cases.

The dipolar hard sphere potential is

$$\phi(12) = \phi_{HS}(r) + \phi_{DD}(12) , \tag{21}$$

where

$$\phi_{HS}(r) = \infty , \quad r < \sigma$$
$$= 0 , \quad r > \sigma \tag{22}$$

for hard spheres of diameter σ, and where the dipole–dipole part $\phi_{DD}(12)$ has axial coefficients

$$\phi_{110}(r) = -\frac{2}{3}\frac{\mu^2}{r^3} ,$$
$$\phi_{111}(r) = \phi_{11-1}(r) = -\frac{1}{3}\frac{\mu^2}{r^3} , \tag{23}$$

with μ the dipole moment. The leading nonvanishing axial coefficients of, say, $S(12)$ are then (arranged in $\mathbf{S}_m$ matrix format):

$$\begin{array}{ccccc}
S_{000} & \cdots & S_{200} & \cdots & S_{400} \\
 & S_{110} & \cdots & S_{310} & \cdots \\
 & & S_{220} & \cdots & S_{420} \\
 & & & S_{330} & \cdots \\
 & & & & S_{440} \\
S_{111} & \cdots & S_{311} & \cdots & \\
 & S_{221} & \cdots & S_{421} & \\
 & & S_{331} & \cdots & \\
 & & & S_{441} & \\
 & S_{222} & \cdots & S_{422} & \\
 & & S_{332} & \cdots & \\
 & & & S_{442} & \\
 & & S_{333} & \cdots & \\
 & & & S_{443} & \\
 & & & S_{444} &
\end{array} .$$

By symmetry, $S_{l_1l_2m}(r) = S_{l_2l_1m}(r) = S_{l_1l_2\bar{m}}(r)$ for the nonvanishing coefficients, so the displayed elements are the only independent ones through index 4. The number of coefficients employed in the calculation is determined by the choice of the largest value of m to be used; for max $m = 0,1,2,3,4,...$ we need, respectively, 1,3,7,13,22,...

coefficients (the cumulative sum in the successive columns above). Our calculation can use all the displayed coefficients; in practice, we find the set of 13 for max $m = 3$ to be entirely adequate, as did Fries and Patey[9] for their similar calculation.

The reference system from which $B_0(r)$ is obtained for use in Eq. (3) is here the hard sphere fluid, as modeled by Verlet–Weis[15] and Henderson–Grundke,[16] for spheres of diameter σ_0. The choice $\sigma_0 = \sigma$ constitutes the usual RHNC approximation.[1] The reference system can be optimized, however, by treating σ_0 as a variable parameter[2] and requiring that its choice satisfy the constraint[3,5]

$$\rho \int d\mathbf{r}[g_{000}(r) - g_0(r)]\sigma_0 \frac{\partial B_0(r)}{\partial \sigma_0} = 0 , \tag{24}$$

where $g_{000}(r)$ is the radial part of the dipolar hard spheres PDF and $g_0(r)$ the reference PDF. This condition for σ_0 has two effects. First, it minimizes the free energy functional associated with the RHNC equation and, second, it removes the inconsistency, otherwise present in the RHNC approximation, between the pressure obtained by differentiation of the free energy and that obtained from the virial theorem. For simple fluids, Eq. (24) is further found in practice to improve the computed results.[3,4]

General expressions[12] for the internal energy U and the pressure p become, for dipolar hard spheres,

$$\beta U/N = 2\pi\rho \int_0^\infty dr\, r^2 [g_{110}(r)\beta\phi_{110}(r) + 2g_{111}(r)\beta\phi_{111}(r)] \tag{25}$$

and

$$\beta p/\rho = 1 + \tfrac{2}{3}\pi\rho\sigma^3 g_{000}(\sigma) + \beta U/N , \tag{26}$$

while the isothermal compressibility χ is given by the usual expression

$$\rho k_B T\chi = \left[1 - 4\pi\rho \int_0^\infty dr\, r^2 C_{000}(r)\right]^{-1} . \tag{27}$$

The RHNC equation provides the free energy A in the form[11]

$$\beta A/N = \beta A_0/N + (\beta\Delta A/N - \beta\Delta A_0/N) , \tag{28}$$

where A_0 is the reference system free energy and

$$\beta\Delta A/N = \tfrac{1}{2}[(\rho k_B T\chi)^{-1} - 1] - \frac{1}{2\rho}\int \frac{d\mathbf{k}}{(2\pi)^3}\left\{\sum_m [\ln\det(\mathbf{I} + (-1)^m\rho\tilde{\mathbf{h}}_m(k)) - (-1)^m\rho\,\mathrm{Tr}\,\tilde{\mathbf{h}}_m(k)] + \rho^2 \sum_{l_1 l_2 m} \tilde{h}_{l_1 l_2 m}(k)[\tfrac{1}{2}\tilde{h}_{l_1 l_2 m}(k) - \tilde{S}_{l_1 l_2 m}(k)]\right\} \tag{29}$$

$$\beta\Delta A_0/N = \tfrac{1}{2}[(\rho k_B T\chi_0)^{-1} - 1] - \frac{1}{2\rho}\int \frac{d\mathbf{k}}{(2\pi)^3}\{\ln[1 + \rho\tilde{h}_0(k)] - \rho\tilde{h}_0(k) + \rho^2\tilde{h}_0(k)[\tfrac{1}{2}\tilde{h}_0(k) - \tilde{S}_0(k)]\} . \tag{30}$$

In Eq. (29), $\tilde{\mathbf{h}}_m(k)$ is the matrix with elements $\tilde{h}_{l_1 l_2 m}(k)$, $l_1, l_2 \geq m$, while det and Tr are the determinant and trace operations. Equation (30) is the reference system version of Eq. (29), which in the present calculation involves just radial functions.

Finally, of particular interest for the dipolar system is the dielectric constant ϵ. For infinite samples, it is obtained equivalently from the Kirkwood formula[17–19]

$$\frac{(\epsilon - 1)(2\epsilon + 1)}{9\epsilon} = yg , \tag{31}$$

with $y = 4\pi\rho\beta\mu^2/9$ and

$$g = 1 + \tfrac{1}{3}\rho\tilde{h}^{110}(0) , \tag{32}$$

and from the asymptotic form[18,19]

$$h^{112}(r) \sim \frac{(\epsilon - 1)^2}{4\pi\rho\epsilon y r^3} . \tag{33}$$

In these expressions, we have introduced variants of the space-fixed coefficients defined by the CG transformation, Eq. (12) to conform with common usage. Specifically, we have

$$h^{110}(r) = -3^{1/2}h(r;110) = h_{110}(r) - 2h_{111}(r) ,$$
$$h^{112}(r) = (\tfrac{3}{2})^{1/2}h(r;112) = h_{110}(r) + h_{111}(r) , \tag{34}$$

and similarly for the transforms. [These functions have also been called $h_\Delta(r)$ and $h_D(r)$, respectively, in many works.] As noted, Eqs. (31) and (33) should produce the same value for the dielectric constant, which provides a useful internal check on the calculation. [For large values of μ, however, Eq. (31) is the more reliable numerically.] It should be remarked that the transform at $k = 0$ in Eq. (32) must be calculated from those of the corresponding $\tilde{C}^{110}(0)$ and $\tilde{S}^{110}(0)$ obtained by step (vi) of the procedure outlined above; the *direct* evaluation of $\tilde{h}^{110}(0)$ by integrating over $h^{110}(r)$ is numerically unreliable. This is especially true for the truncated potential discussed next.

Simulation methods using toroidal boundary conditions[8] must, as noted earlier, use potentials of finite range, enforced by truncation if necessary. The reaction field method of Barker and Watts[20] is an attempt to heal the effects of this cutoff of the dipolar potential that is equivalent[21] to an effective dipole–dipole interaction with axial coefficients

$$\phi^{\mathrm{eff}}_{110}(r) = \phi_{110}(r) - \frac{f\mu^2}{3R_c^3} ,$$
$$\phi^{\mathrm{eff}}_{111}(r) = \phi_{111}(r) + \frac{f\mu^2}{3R_c^3} , \quad r < R_c \tag{35}$$

and

TABLE I. Thermodynamics of the dipolar hard spheres fluid at $\rho\sigma^3 = 0.8$ with no truncation of the potential. Results with $\sigma_0/\sigma = 1$ are from the RHNC equation; those with $\sigma_0/\sigma < 1$ are from the optimized RHNC equation satisfying Eq. (24).

$\beta\mu^2/\sigma^3$	σ_0/σ	$\beta U/N$	$\beta p/\rho$	$\rho k T_B \chi$	$\beta A/N$	ϵ
0.5	1.0	−0.326	7.47	0.0373	3.22	3.70
1.0	1.0	−0.972	7.01	0.0385	2.81	8.83
1.0	0.9978	−0.973	7.07	0.0389	2.81	8.83
1.5	1.0	−1.75	6.50	0.0399	2.27	17.4
1.5	0.9948	−1.75	6.62	0.0410	2.27	17.3
2.0	1.0	−2.61	5.96	0.0416	1.66	31.8
2.0	0.9915	−2.62	6.17	0.0435	1.65	31.8
2.25	1.0	−3.07	5.69	0.0426	1.32	43.3
2.25	0.9898	−3.08	5.95	0.0449	1.31	43.1
2.50	1.0	−3.54	5.41	0.0436	0.979	60.5
2.50	0.9878	−3.55	5.72	0.0465	0.975	60.4
2.75	1.0	−4.03	5.13	0.0449	0.620	91.8
2.75	0.9860	−4.04	5.49	0.0483	0.617	91.7

$$\phi_{110}^{\text{eff}}(r) = 0\,,$$

$$\phi_{111}^{\text{eff}}(r) = 0\,, \quad r > R_c\,,$$

where

$$f = \frac{2(\epsilon_{\text{RF}} - 1)}{2\epsilon_{\text{RF}} + 1}\,, \tag{36}$$

and R_c is the cutoff separation, while ϵ_{RF} is the dielectric constant of the infinite continuum surrounding the truncation sphere. For this interaction, Eq. (33) is no longer valid and Eq. (31) must be replaced with[7,8]

$$\frac{(\epsilon - 1)(2\epsilon_{\text{RF}} + 1)}{3(\epsilon + 2\epsilon_{\text{RF}})} = yg\,, \tag{37}$$

with g still determined by Eq. (32). The other thermodynamic formulas are not affected by this change, with the exception of the pressure, which picks up an additional contribution from the new delta function in $\phi'(12)$ at $r = R_c$. This is a small effect which has been included in the data reported below. The new discontinuities in $C(12)$ and $g(12)$ at $r = R_c$ also call for special treatment in integrals such as those of steps (iii) and (iv).

III. RESULTS

The iterative solutions were typically started from the converged solution of a neighboring thermodynamic state and continued until the largest difference between successive iterates of $rS_{l_1 l_2 m}(r)$ was less than 10^{-3} for all 13 coefficients used. With Gillan's method[13] accelerating the convergence of $S_{000}(r)$, the last coefficient to converge was generally $S_{110}(r)$. To ensure a sufficient range, we used $N_r = 1024$ points with an interval $\Delta r = 0.02\sigma$ in the solutions with the complete dipolar potential. With the truncated potential, an adequate range is more of a problem and the number of points was doubled to 2048 with the same grid size. The Gaussian quadratures of step (i) were done with $n = 10$.

The computed thermodynamic properties of the dipolar hard sphere fluid at density $\rho\sigma^3 = 0.8$ are shown in Table I for seven values of the reduced dipole moment. Results from both the usual RHNC equation ($\sigma_0 = \sigma$) and the optimized RHNC equation ($\sigma_0 < \sigma$) are given, with the value of σ_0 needed to satisfy Eq. (24) also tabulated. The greatest effect of the optimization is on the radial functions, which is reflected here in the larger changes it produces in the computed pressure and compressibility. The dielectric constant, on the other hand, is scarcely affected. The first few axial projections of $g(12)$ and $\tilde{h}(12)$ are shown, respectively, in Fig. 1 and as the solid curves in Fig. 2 for the (optimized) case at $\rho\sigma^3 = 0.8$ and $\beta\mu^2/\sigma^3 = 2.0$.

Computed properties for the *truncated* potential, Eq. (35), with $R_c = 4.5\sigma$ and $\epsilon_{\text{RF}} = 50$, obtained from the optimized RHNC equation are listed in Table II. There is generally excellent agreement with the corresponding data in Table I, including quite good correspondence of the dielectric constant computed using Eq. (37) with the infinite sample value from Eq. (31) for the first two states of Table II. For the last state with the largest dipole moment there is significant difference in ϵ. To check if this is due to the cutoff

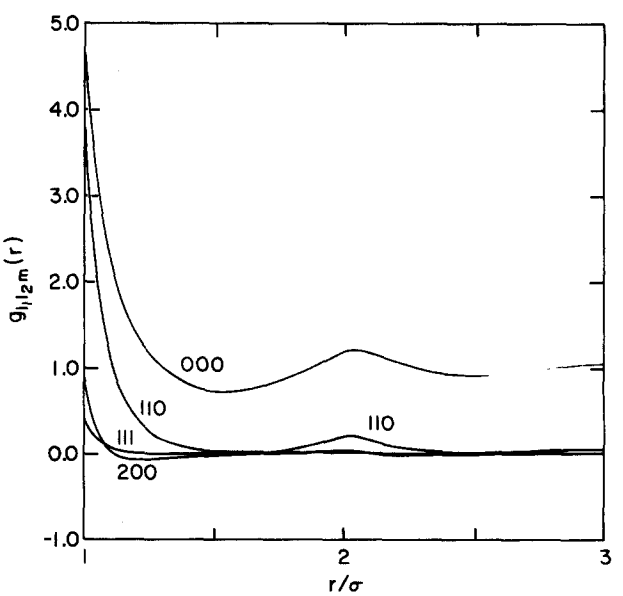

FIG. 1. Axial coefficients of $g(12)$ for the dipolar hard spheres fluid at $\rho\sigma^3 = 0.8$ and $\beta\mu^2/\sigma^3 = 2.0$, obtained from the optimized RHNC equation. Results for the complete and truncated potentials are identical on this scale.

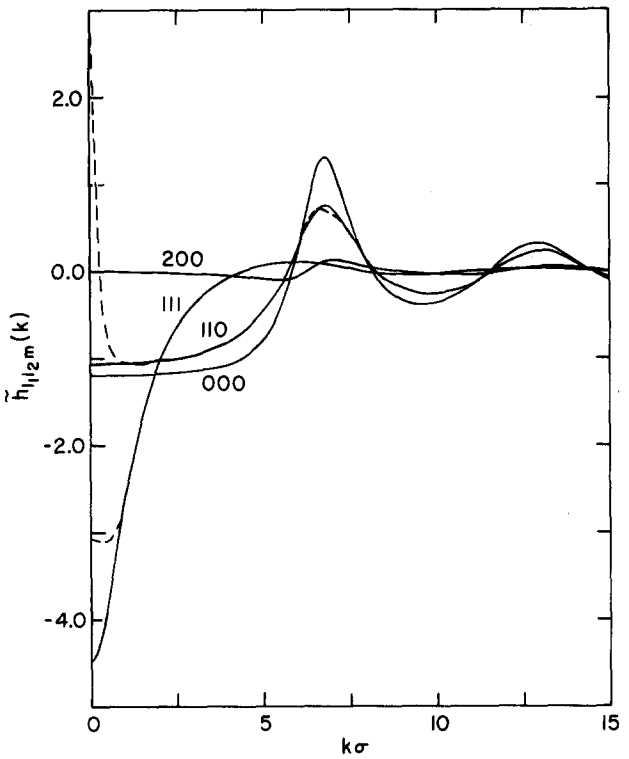

FIG. 2. Axial coefficients of $\tilde{h}(12)$ for the dipolar hard spheres fluid at $\rho\sigma^3 = 0.8$ and $\beta\mu/\sigma^3 = 2.0$, obtained from the optimized RHNC equation. The solid curves are for the potential with no truncation, dashed curves for the potential with reaction field truncation.

separation of 4.5σ becoming more inadequate as μ increases, as seemed likely, we have recomputed this state using $R_c = 6.0\sigma$ with other parameters unchanged. The effect of this on ϵ is indeed large and is seen to move the finite sample value much closer to the bulk value. Such an increase in R_c would require roughly a doubling of the sample size (number of molecules) in a computer simulation.

While the reaction field correction does produce a dielectric constant in consonance with that of an infinite sample, the long-range behavior of the correlation functions for the truncated potential is nevertheless anomalous. This would not at all be evident on the scale of Fig. 1, which indeed could as well be that of the truncated potential data. It shows up strikingly, however, in the short-range behavior of some Fourier transforms, as seen in Fig. 2, where the dashed curves are for the RF potential. For very small k, the axial coefficients most significant for the dipole potential,

TABLE II. Thermodynamics of the dipolar hard spheres fluid at $\rho\sigma^3 = 0.8$, with reaction field truncation of the potential, obtained from the optimized RHNC equation. Two truncation distances R_c were used for the last state.

$\beta\mu^2/\sigma^3$	R_c/σ	$\beta U/N$	$\beta p/\rho$	$\rho k_B T\chi$	$\beta A/N$	ϵ
1.0	4.5	−0.969	7.06	0.0389	2.81	8.74
2.0	4.5	−2.61	6.16	0.0434	1.65	30.5
2.75	4.5	−4.03	5.47	0.0479	0.619	76.8
2.75	6.0	−4.05	5.47	0.0483	0.608	91.1

$\tilde{h}_{110}(k)$ and $\tilde{h}_{111}(k)$, are clearly distorted by the potential truncation.

Fries and Patey[9] have reported values of 8.82, 31.7, and 93.0 for ϵ and −0.98, −2.62, and −4.04 for $\beta U/N$ at $\rho\sigma^3 = 0.8$ and $\beta\mu^2/\sigma^3 = 1.0$, 2.0, and 2.75, respectively, obtained from the RHNC equation for the infinite system. These results are in excellent agreement with our data in Table I.

ACKNOWLEDGMENTS

This work was supported by the National Science Foundation under Grant No. CHE-8402144 (F.L.) and by the U.S.–Spain Joint Committee for Scientific and Technological Cooperation under Grant No. CCB-8409015.

[1]F. Lado, Phys. Rev. A **8**, 2548 (1973).
[2]Y. Rosenfeld and N. W. Ashcroft, Phys. Rev. A **20**, 1208 (1979).
[3]F. Lado, Phys. Lett. A **89**, 196 (1982).
[4]F. Lado, S. M. Foiles, and N. W. Ashcroft, Phys. Rev. A **28**, 2374 (1983).
[5]F. Lado, J. Chem. Phys. **81**, 4592 (1984).
[6]See, e.g., the excellent review by G. Stell, G. N. Patey, and J. S. Høye, Adv. Chem. Phys. **38**, 183 (1981), and references therein.
[7]G. N. Patey, D. Levesque, and J. J. Weis, Mol. Phys. **45**, 733 (1982).
[8]M. Neumann, Mol. Phys. **50**, 841 (1983).
[9]P. H. Fries and G. N. Patey, J. Chem. Phys. **82**, 429 (1985).
[10]F. Lado, Mol. Phys. **47**, 283 (1982).
[11]F. Lado, Mol. Phys. **47**, 299 (1982).
[12]W. B. Streett and K. E. Gubbins, Ann. Rev. Phys. Chem. **28**, 373 (1977).
[13]M. J. Gillan, Mol. Phys. **38**, 1781 (1979).
[14]A. A. Broyles, J. Chem. Phys. **33**, 456 (1960).
[15]L. Verlet and J. J. Weis, Phys. Rev. A **5**, 939 (1972).
[16]D. Henderson and E. W. Grundke, J. Chem. Phys. **63**, 601 (1975).
[17]J. G. Kirkwood, J. Chem. Phys. **7**, 911 (1939).
[18]G. Nienhuis and J. M. Deutch, J. Chem. Phys. **55**, 4213 (1971); **56**, 235 (1972).
[19]J. S. Høye and G. Stell, J. Chem. Phys. **61**, 562 (1974); **64**, 1952 (1976).
[20]J. A. Barker and R. O. Watts, Mol. Phys. **26**, 789 (1973); R. O. Watts, *ibid.* **28**, 1069 (1974).
[21]M. Neumann and O. Steinhauser, Mol. Phys. **39**, 437 (1980).